Cavity design and characteristics of monolithic long-wavelength InAs/InP quantum dash passively mode-locked lasers

C.-Y. Lin[1*], Y.-C. Xin[2], Y. Li[1], F. L. Chiragh[1] and L. F. Lester[1]

[1]*University of New Mexico, Center for High Technology Materials, 1313 Goddard SE, Albuquerque, NM 87106, USA*
[2]*IBM Systems &Technology Group, Semiconductor Solutions, 2070 Route 52 Hopewell Junction, NY 12533, USA*
**cylin@unm.edu*

Abstract: By extending the net-gain modulation phasor approach to account for the discrete distribution of the gain and saturable absorber sections in the cavity, a convenient model is derived and experimentally verified for the cavity design of two-section passively mode-locked quantum dash (QDash) lasers. The new set of equations can be used to predict functional device layouts using the measured modal gain and loss characteristics as input. It is shown to be a valuable tool for realizing the cavity design of monolithic long-wavelength InAs/InP QDash passively mode-locked lasers.

©2009 Optical Society of America

OCIS codes: (140.4050) Mode-locked lasers; (140.5960) Semiconductor lasers; (130.3120) Integrated optics devices.

References and links

1. D. A. B. Miller, “Rationale and challenges for optical interconnects to electronic chips,” Proc. IEEE **88**(6), 728–749 (2000).
2. G. A. Keeler, B. E. Nelson, D. Agarwal, C. Debaes, N. C. Helman, A. Bhatnagar, and D. A. B. Miller, “The benefits of ultrashort optical pulses in optically interconnected systems,” IEEE J. Sel. Top. Quantum Electron. **9**(2), 477–485 (2003).
3. Y.-C. Xin, Y. Li, V. Kovanis, A. L. Gray, L. Zhang, and L. F. Lester, “Reconfigurable quantum dot monolithic multisection passive mode-locked lasers,” Opt. Express **15**(12), 7623–7633 (2007).
4. M. Kuntz, G. Fiol, M. Lämmlin, D. Bimberg, M. G. Thompson, K. T. Tan, C. Marinelli, A. Wonfor, R. Sellin, R. V. Penty, I. H. White, V. M. Ustinov, A. E. Zhukov, Y. M. Shernyakov, A. R. Kovsh, N. N. Ledentsov, C. Schubert, and V. Marembert, “Direct modulation and mode locking of 1.3 μm quantum dot lasers,” N. J. Phys. **6**, 181 (2004).
5. E. U. Rafailov, M. A. Cataluna, and W. Sibbett, “Mode-locked quantum-dot lasers,” Nat. Photonics **1**(7), 395–401 (2007).
6. M. G. Thompson, A. R. Rae, M. Xia, R. V. Penty, and I. H. White, “InGaAs quantum-dot mode-locked laser diodes,” IEEE J. Sel. Top. Quantum Electron. **15**, 661–672 (2009).
7. M. J. R. Heck, E. A. J. M. Bente, B. Smalbrugge, Y. S. Oei, M. K. Smit, S. Anantathanasarn, and R. Nötzel, “Observation of Q-switching and mode-locking in two-section InAs/InP (100) quantum dot lasers around 1.55 mum,” Opt. Express **15**(25), 16292–16301 (2007).
8. F. Lelarge, B. Dagens, J. Renaudier, R. Brenot, A. Accard, F. Dijk, D. Make, O. L. Gouezigou, J.-G. Provost, F. Poingt, J. Landreau, O. Drisse, E. Derouin, B. Rousseau, F. Pommereau, and G.-H. Duan, “Recent advances on InAs/InP quantum dash based semiconductor lasers and optical amplifiers operating at 1.55 μm,” IEEE J. Sel. Top. Quantum Electron. **13**(1), 111–124 (2007).
9. D. Zhou, R. Piron, M. Dontabactouny, O. Dehaese, F. Grillot, T. Batte, K. Tavernier, J. Even, and S. Loualiche, “Low threshold current density of InAs quantum dash laser on InP (100) through optimizing double cap technique,” Appl. Phys. Lett. **94**(8), 081107 (2009).
10. G. T. Liu, A. Stintz, H. Li, K. J. Malloy, and L. F. Lester, “Extremely Low Room-Temperature Threshold Current Density Diode Lasers Using InAs Dots in an $In_{0.15}Ga_{0.85}As$ Quantum Well,” Electron. Lett. **35**(14), 1163–1165 (1999).
11. K. Y. Lau, and J. Paslaski, “Condition for short pulse generation in ultrahigh frequency mode-locking of semiconductor-Lasers,” IEEE Photon. Technol. Lett. **3**(11), 974–976 (1991).
12. J. Palaski, and K. Y. Lau, “Parameter ranges for ultrahigh frequency mode-locking of semiconductor lasers,” Appl. Phys. Lett. **59**(1), 7–9 (1991).
13. Y.-C. Xin, Y. Li, A. Martinez, T. J. Rotter, H. Su, L. Zhang, A. L. Gray, S. Luong, K. Sun, Z. Zou, J. Zilko, P. M. Varangis, and L. F. Lester, “Optical gain and absorption of quantum dots measured using an alternative segmented contact method,” IEEE J. Quantum Electron. **42**(7), 725–732 (2006).

#113021 - $15.00 USD Received 18 Jun 2009; revised 15 Sep 2009; accepted 6 Oct 2009; published 16 Oct 2009

14. P. Blood, G. M. Lewis, P. M. Smowton, H. Summers, J. Thomson, and J. Lutti, "Characterization of semiconductor laser gain media by the segmented contact method," IEEE J. Sel. Top. Quantum Electron. **9**(5), 1275–1282 (2003).
15. N. G. Usechak, Y.-C. Xin, C.-Y. Lin, L. F. Lester, D. J. Kane, and V. Kovanis, "Modeling and direct electric-field measurements of passively mode-locked quantum-dot lasers," IEEE J. Sel. Top. Quantum Electron. **15**, 653–660 (2009).
16. A. G. Vladimirov, and D. Turaev, "Model for passive mode locking in semiconductor lasers," Phys. Rev. A **72**(3), 033808 (2005).
17. P. Vasilev, *Mode-locking Diode Lasers, Ultrafast diode lasers Fundamentals and applications,* (Artech House, Boston 1995), Chap. 4.
18. Y.-C. Xin, C.-Y. Lin, Y. Li, H. P. Bae, H. B. Yuen, M. A. Wistey, J. S. Harris, S. R. Bank, and L. F. Lester, "Monolithic 1.55 µm GaInNAsSb quantum well passively modelocked lasers," Electron. Lett. **44**(9), 581–582 (2008).
19. C.-Y. Lin, Y.-C. Xin, N. A. Naderi, F. L. Chiragh, and L. F. Lester, "Monolithic 1.58-micron InAs/InP quantum dash passively mode-locked lasers," Proc. SPIE **7211**, 721118 (2009).
20. F. Grillot, C.-Y. Lin, N. A. Naderi, M. Pochet, and L. F. Lester, "Optical feedback instabilities in a monolithic InAs/GaAs quantum dot passively mode-locked laser," Appl. Phys. Lett. **94**(15), 153503 (2009).
21. R.-H. Wang, A. Stintz, P. M. Varangis, T. C. Newell, H. Li, K. J. Malloy, and L. F. Lester, "Room-temperature operation of InAs quantum-dash lasers on InP (001)," IEEE Photon. Technol. Lett. **13**(8), 767–769 (2001).
22. N. Naderi, M. Pochet, F. Grillot, N. Terry, V. Kovanis, and L. F. Lester, "Modeling the injection-locked behavior of a quantum dash semiconductor laser," IEEE J. Sel. Top. Quantum Electron. **15**, 563–571 (2009).

1. Introduction

Monolithic mode-locked lasers (MLLs) are promising candidates for inter-chip/intra-chip clock distribution as well as high bit-rate optical time division multiplexing, electro-optic sampling, and arbitrary waveform generation due to their compact size, low power consumption, and direct electrical pumping [1,2]. Some unique characteristics of quantum dot (QD) materials, such as ultra broad bandwidth, ultra fast gain dynamics, and easily saturated gain and absorption, make them an ideal choice for semiconductor monolithic MLLs. For QD systems, the most impressive results that clearly demonstrate complete mode-locking have been realized for 1.2-1.3 µm QD MLLs fabricated on a GaAs substrate [3–6]. Although QD and quantum dash (QDash) MLLs made on InP substrates in the 1.55-µm range have been vigorously pursued, achieving mode-locking in two-section devices using these materials has been more challenging [7,8]. In part, it is believed that this is caused by the higher threshold current density and waveguide internal loss in InP-based QDs and QDashes compared to the more mature InAs/GaAs QD material system [9,10]. To further improve the development of 1.55-µm passive QD/QDash MLLs, a simple analytical model is needed to provide cavity geometry guidelines that can improve the mode locking performance in two-section devices.

This work extends a previous model based on a microwave photonics perspective that treated passive mode-locking without self-pulsation using a net-gain modulation phasor approach [11,12]. The new set of equations presented here includes the influence of the waveguide internal loss and the effect of separate as opposed to distributed gain and loss. We theoretically predict and experimentally confirm the passive MLL geometries using material gain and loss data that are obtained through the segmented contact method [13,14]. Compared to our previous delay differential equation model [15] and the work of Vladimirov and Turaev [16], the advantage of the proposed analytical model is the prediction of the functional mode-locking device layout through the use of measured static laser parameters *on the actual device*. Thus, we can construct a simpler analytical model without knowing the material parameters such as the carrier lifetime or the gain/absorber recovery times. The theory is applied to the design of monolithic InAs/InP QDash passive MLLs emitting at 1.59-µm. Mode locking is achieved as predicted, and a repetition rate as high as 18.4 GHz is realized.

2. Theory

A frequently cited condition for passive mode-locking requires that the stability parameter, S, must be greater than 1:

#113021 - $15.00 USD Received 18 Jun 2009; revised 15 Sep 2009; accepted 6 Oct 2009; published 16 Oct 2009
(C) 2009 OSA

$$S = \frac{E_{sat,g}}{E_{sat,abs}} = \frac{hvA / G_g}{hvA / G_a} = \frac{G_a}{G_g} > 1 \qquad (1)$$

where $E_{sat,abs}$ is the saturation energy of the absorber, $E_{sat,g}$ is the saturation energy for the gain section, h is Planck's constant, v is the optical frequency, G_g is the differential gain in the gain section multiplied by the group velocity, G_a is the differential loss in the absorber multiplied by the group velocity and A is the optical mode cross-sectional area, which is equal in the absorber and gain sections of the monolithic semiconductor laser [17]. However, this requirement is not stringent and rarely used to guide semiconductor MLL cavity design. Using a net-gain modulation phasor approach, Lau and Paslaski derived a more useful guideline for obtaining passive mode-locking instead of self-pulsation in the region near lasing threshold where the two processes typically compete and the pulse width is typically the shortest [11,12].

This model, however, was based on the assumption that the gain and the saturable absorber are distributed *uniformly* in the optical cavity, not in separate electrically-isolated sections as common done, and the internal loss was not considered. In the QDash material system, the gain and absorption per unit length are much smaller compared to those of a quantum well or bulk semiconductor system. Thus, we can approximate the actual lumped gain and absorber sections of the optical waveguide as an average gain and loss that are distributed uniformly. It is also important to include the internal loss effect in QDash material system due to the comparable value to the unsaturated absorption. Based on these approximations, we have extended Lau and Paslaski's model to a two-section MLL device geometry that includes a gain section of length L_g and an absorber section of length L_a, and have accounted for the internal loss, α_i, in the optical waveguide.

To understand the region of mode locking without self-pulsation, we employ the net-gain modulation phasor analysis [11,12]. In this approach, the photon intensity oscillation is represented by $s \cdot e^{i\omega t}$, where s is the real amplitude of the oscillation. ω = Ω_{MLL}= the longitudinal mode spacing or mode-locking frequency. The net gain modulation represents the difference between the average gain and the average loss modulation in the gain and absorber media. Following Lau and Paslaski's model and accounting for the distribution of the gain and absorption in separate sections of the cavity, we write the modified net gain modulation equation for a two-section passive MLL as [12]:

$$\begin{aligned} & g_{net} = \left\{ \frac{-G_g g_0 L_g}{i\omega + 1/T_g} - \frac{-G_a a_0 L_a}{i\omega + 1/T_a} \right\} \frac{se^{i\omega t}}{L} = \hat{g}_{net} e^{i\omega t} \\ & 1/T_g = 1/\tau_g + G_g S_0 \qquad 1/T_a = 1/\tau_a + G_a S_0 \\ & G_g = v_g \frac{dg_0}{dn} \qquad G_a = v_g \frac{da_0}{dn} \end{aligned} \qquad (2)$$

$\hat{g}_{net}$ is a phasor quantity which is responsible for driving the optical modulation. In Eq. (2), g_0 is the modal gain in the gain section and a_0 is the unsaturated absorption in the absorber region. L is the cavity length and $L=L_a+L_g$; v_g and n are the group velocity and the carrier density, respectively. $1/Tg$ is the carrier recombination rate in the gain section consisting of the sum of the spontaneous rate, $1/\tau_g$, and the stimulated rate G_gS_0. $1/T_a$ is the carrier removal rate in the absorber consisting of the sum of the spontaneous rate, $1/\tau_a$, and the stimulated rate, G_aS_0. τ_g and τ_a are the spontaneous carrier lifetimes in the gain and absorber regions, respectively, and should not be confused with the recovery times. The first quantity in { } in Eq. (2) is related to the average gain modulation, and the second quantity represents the average loss modulation.

#113021 - $15.00 USD Received 18 Jun 2009; revised 15 Sep 2009; accepted 6 Oct 2009; published 16 Oct 2009
(C) 2009 OSA

The s in Eq. (2) is related to the modulation depth which is assumed to be 100% so that $s = S_0 / 2$. S_0 is the average photon density in the cavity:

$$S_0 = \frac{1}{\alpha_m \upsilon_g h\nu} \frac{\Gamma P}{WdL} \tag{3}$$

where α_m is the mirror loss, P is the peak optical power, $h\nu$ is the photon energy, W is the lateral mode width, and Γ is the optical confinement factor.

The necessary conditions for mode-locking without self-pulsation are that the repetition rate should be much faster than the stimulated rate, i.e., $\omega = \Omega_{MLL} = v_g/2L$ $\omega = \Omega_{MLL} = \upsilon_g / 2L >> G_{g/a} S_0$ and the stimulated rates are much greater than the spontaneous recombination rates in the gain and absorber section, i.e., $G_g S_0 >> 1/\tau_g$ and $G_a S_0 >> 1/\tau_a$ [12]. In this work, we further require that the real part of the net gain modulation must exceed the internal loss, α_i, of the waveguide:

$$\left(-G_g^2 g_0 \frac{L_g}{L} + G_a^2 a_0 \frac{L_a}{L} \right) \frac{S_0^2}{2\Omega_{MLL}^2} > \alpha_i \tag{4}$$

then:

$$\left(\frac{da_0}{dn} \right)^2 a_0 \frac{L_a}{L} - \left(\frac{dg_0}{dn} \right)^2 g_0 \frac{L_g}{L} > \frac{\alpha_i}{2} \left(\alpha_m v_g \frac{Wd}{\Gamma P} h\nu \right)^2 \tag{5}$$

Inequality (5) gives the necessary operating condition for a two-section passive MLL and highlights the interdependence of the material parameters and the device's 2-section structure. To apply Eq. (5) to the design of an MLL cavity, we make approximations under two different conditions. First, we assume that the differential gain is much smaller than the differential absorption: $G_a >> G_g$ or, equivalently, that the gain section is biased under strong population inversion. Since it is difficult to measure the differential gain and absorption with respect to the carrier density in practice, dg_0 /dn is replaced with dg_0 /dJ and Eq. (5) can be approximated by [19]:

$$\left(\left. \frac{dg_0}{dJ} \right|_{g_0=0} \right)^2 \frac{a_0}{\alpha_i} > \frac{L}{2L_a} \left(\eta_i \tau \frac{\alpha_m W v_g}{\Gamma P} \frac{h\nu}{q} \right)^2 \tag{6}$$

Here J is the current density, τ is the carrier lifetime, and η_i is the injection efficiency of the laser. We also conservatively approximate that $da_0 / dn \approx dg_0 / dn\big|_{g_0=0}$. The left-hand-side of Eq. (6) emphasizes that a high contrast between the unsaturated absorption, a_0, and the internal loss, α_i, is favorable for mode-locking. In addition, upon measuring the various device and material parameters, we can use Eq. (6) to predict cavity designs (L_a and L_g) for two-section mode-locked lasers of a desired repetition rate using novel active region materials. This is the situation described below for the QDash lasers. Alternatively, we can rearrange Eq. (6) to estimate the minimum required peak power level according to the following expression:

$$P > \sqrt{\frac{L\alpha_i}{2L_a a_0}} \left[\eta_i \tau \frac{\alpha_m W v_g}{\Gamma \left(dg_0/dJ\big|_{g_0=0} \right)} \frac{h\nu}{q} \right] \tag{7}$$

Equation (7) reinforces the idea that the internal loss is detrimental to mode-locking in a semiconductor laser by requiring a high power for the onset of operation.

Although it is possible to measure the variables in Eq. (6)-(7) for the *actual* mode-locked laser or test structures associated with it, the carrier lifetime is frequently difficult to obtain. Thus, a further assumption can be made to obtain a simpler analytical guideline. The second approximation assumes that the power is sufficiently large that the right-hand-side of Eq. (6)

#113021 - $15.00 USD Received 18 Jun 2009; revised 15 Sep 2009; accepted 6 Oct 2009; published 16 Oct 2009
(C) 2009 OSA

is negligible. In this case, the following condition analogous to that found in [11,12] is obtained:

$$\frac{a_0}{g_0}\frac{L_a}{L_g} > \left(\frac{\dfrac{dg_0}{dJ}}{\left.\dfrac{dg_0}{dJ}\right|_{g_0=0}} \right)^2 \tag{8}$$

From Eq. (8) it is found that a longer absorber is desirable for realizing mode-locking, especially when the differential gain is not much smaller than the differential absorption. Similar to Eq. (1), Eq. (8) also suggests that the design strategy of a passive MLL is to minimize the ratio of the differential gain to differential absorption.

The threshold condition in the laser cavity, Eq. (9), is another constraint on the system and is applied to determine the modal gain, g_0.

$$g_0 L_g = a_0 L_a + (\alpha_m + \alpha_i) L \tag{9}$$

Therefore, provided that the measured modal gain and loss data is also available from the segmented test structure that is integrated into the MLL, possible cavity designs can be explored using Eq. (8) before even fabricating them. These analytical guidelines have been successfully applied previously [18–20], but the range of designs and analysis is expanded in this work verifying the broad applicability of the theory.

3. Material Structure and Characterization

3.1 Material structure

The QDash active region investigated in this work was grown on an n^+-InP substrate [21]. Figure 1 shows the structural diagram of the epitaxial layers. The dashes-in-a-well (DWELL) active region consists of 5 layers of InAs quantum dashes embedded in compressively-strained $Al_{0.20}Ga_{0.16}In_{0.64}As$ quantum wells separated by 30-nm undoped tensile-strained $Al_{0.28}Ga_{0.22}In_{0.50}As$ spacers. A lattice-matched 105-nm thick layer of undoped $Al_{0.30}Ga_{0.18}In_{0.52}As$ is added on each side of the active region. The p-cladding layer is step-doped AlInAs with a thickness of 1.5-µm to reduce free carrier loss. The n-cladding layer is 500-nm thick AlInAs. The laser structure is capped with a 100-nm heavily p-type doped InGaAs layer.

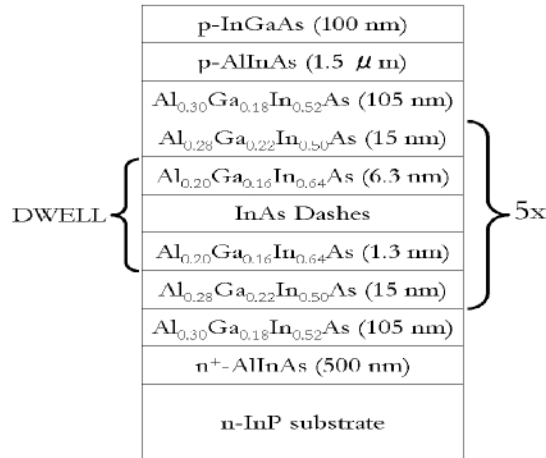

Fig. 1. The layer structure of the InAs QDash laser

#113021 - $15.00 USD Received 18 Jun 2009; revised 15 Sep 2009; accepted 6 Oct 2009; published 16 Oct 2009
(C) 2009 OSA

3.2 Material Characterization and MLL Device Preparation

The optical cavity shares a common 4-µm wide ridge waveguide with 0.5-mm segmented anode contacts that have approximately 1 MΩ electrical isolation between them. First, this layout is used to measure the modal gain and loss characteristics of the InAs QDash active region using an improved segmented contact method [13]. Second, the MLL is built by reconfiguring this same linear array of diodes [4]. Figures 2(a) and (b) show the modal gain and total loss data as a function of the emission wavelength, respectively. The notable features include: 1) the gain and loss are relatively modest and comparable to quantum dot active region values and 2) the long-wavelength limit of the total loss measurement gives an estimate of the internal loss (about 14 cm^{-1}) that is generally more reliable than that derived from efficiency measurements of different cavity length lasers [13,17]. The segmented device is cleaved and configured into an MLL by wire bonding to form a two-section device with separate gain and saturable absorber regions as depicted in Fig. 3. A highly reflective coating (95% reflectivity) is applied to the mirror facet next to the absorber, and the other facet is cleaved (32% reflectivity). All the lasers examined in this study operate at a wavelength of 1.59 µm, which is noticeably longer than the peak gain wavelengths observed in Fig. 2(a). As explained in Fig. 4, which plots a qualitative comparison of the left- and right-hand sides of Eq. (9), this result is due primarily to the rapid rise of the loss with decreasing wavelength as seen experimentally in Fig. 2(b).

Figure 5 presents the modal gain at a wavelength of 1.59-µm as a function of pump current density and derived from Fig. 2(a). The differential gain with respect to current density can be obtained from this figure. It is observed that the modal gain starts to saturate at 21 cm^{-1} for a pump current density over 2.5 kA/cm^2 and with that, consequently, the differential gain decreases rapidly to near zero in this region. As shown in Fig. 5, a unique property of the QDash two-section MLL that we exploit compared to a single-section device is the abrupt gain saturation characteristic of the nanostructure compared to the traditional QW materials. Thus from Eq. (8), QDashes have a significant advantage in achieving stable mode-locking compared to QW-based MLLs.

Based on Eq. (8), it is a reasonable assumption that the device will more easily mode-lock when the current density in the gain section is over 2.5 kA/cm^2. Conversely, at a modal gain value equal to zero, dg_0/dJ is 0.018 cm/A, and the unsaturated absorption at 1 V reverse voltage and 1.59-µm is 17.5 cm^{-1}. The latter is calculated by deducting the internal loss of 14 cm^{-1} from the total loss value at the relevant wavelength. After obtaining the parameters of the MLL cavity, possible geometries for the 1.59-µm InAs/InP passive QDash MLL can be predicted and the robustness of Eq. (8) can be evaluated.

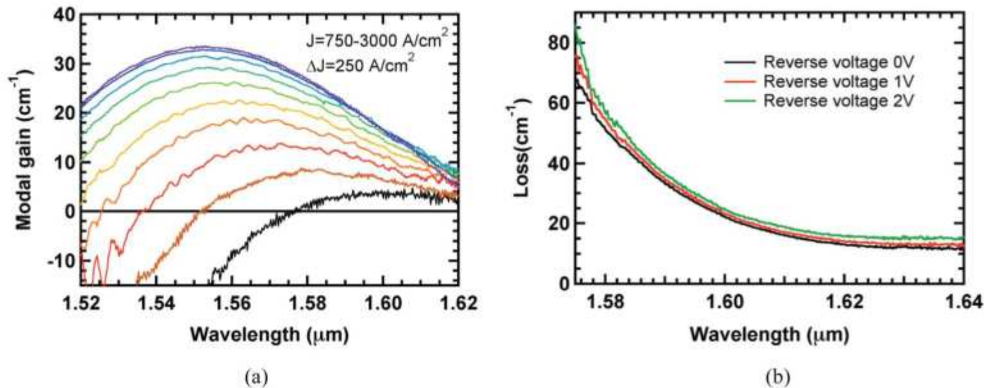

Fig. 2. The room-temperature modal gain (a) and total loss (b) measured using the segmented contact method.

#113021 - $15.00 USD Received 18 Jun 2009; revised 15 Sep 2009; accepted 6 Oct 2009; published 16 Oct 2009
(C) 2009 OSA

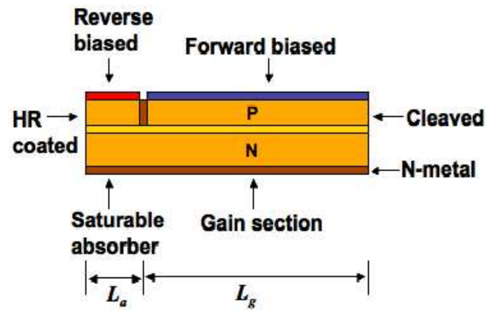

Fig. 3. The side view of the two-section passive QDash MLL.

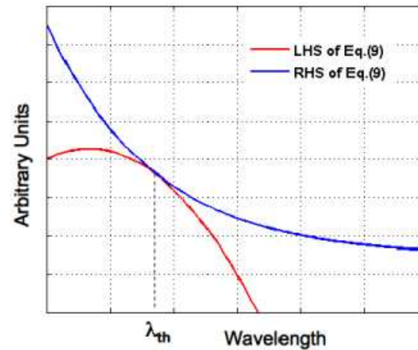

Fig. 4. Qualitative comparison of the left- and right- hand sides of Eq. (9) and the determination of thethreshold wavelength

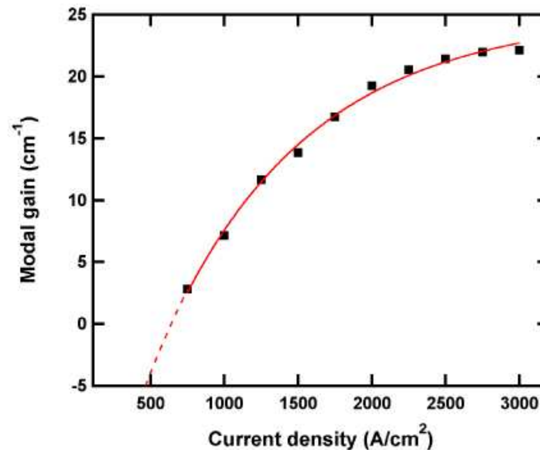

Fig. 5. The modal gain vs. pump current density at the wavelength of 1.59-µm.

4. Device Design and Characterization

According to the model from the previous section, we examined InAs QDash passive MLLs with a total cavity length of 2.3-mm, 3.5-mm, and 4-mm, respectively. For the 2.3-mm cavity length with an absorber of 0.3-mm, the gain section must provide a modal gain, g_0, of 21.8 cm^{-1} at 1.59-µm according to the threshold condition. This value is near to the maximum modal gain value with a corresponding current density of 2750 A/cm^2. The differential gain is 0.0008 cm/A, which is much smaller than the differential loss value. After calculation, the 2.3-mm and 3.5-mm devices satisfy the condition stated in Eq. (8), and it is noteworthy that

#113021 - $15.00 USD Received 18 Jun 2009; revised 15 Sep 2009; accepted 6 Oct 2009; published 16 Oct 2009
(C) 2009 OSA

the 2.3-mm device has a ratio of over 60 comparing the left- and right-hand sides of Eq. (8). In contrast, the 4-mm cavity length MLL does not satisfy Eq. (8). The 2.3-mm and 3.5-mm QDash MLLs are predicted to work under mode-locking operation without self-pulsation and the 4-mm device should not mode-lock at all. The device parameter values and the mode-locking analysis results are summarized in Tables 1 and 2. A 4-mm cavity length device with a 0.5-mm absorber and a 3.5-mm gain section is abbreviated as $A_{0.5}G_{3.5}$.

According to Eq. (7), the minimum peak power required can be estimated as well. Using a carrier lifetime of 170 ps, injection efficiency of 81%, and an optical confinement factor equal to 0.096 [22], the estimated value for the minimum peak power is about 0.6 W for the 3.5-mm QDash MLL. This is a high estimate because of the conservatively low value that is used for the differential absorption, but is reasonable considering typical peak operating powers in quantum dot MLLs [3].

Table 1. Parameter values for the mode-locked laser simulation

	$A_{0.5}G_{3.5}$	$A_{0.5}G_{3.0}$	$A_{0.3}G_{2.0}$
α_m (cm^{-1})	1.48	1.7	2.58
a_0 at 1.59-µm (cm^{-1})	17.5 (Vr=1V)	17.5 (Vr=1V)	18 (Vr=2V)
dg_0/dJ (cm/A)	0.0073	0.0021	0.0008
dg_0/dJ at g_0=0 (cm/A)	0.018	0.018	0.018

Table 2. Mode-locking analysis according to Eq. (1) and (8).

Equation (1) satisfied	Yes	Yes	Yes
Equation (8) satisfied	No	Yes	Strong
Mode-locking operation?	No	Yes	Yes

The figures below show data for the 2.3-mm and 3.5-mm cavity length passive QDash MLLs. Figure 6 is the Light-Current (LI) curve of the laser for various absorber biases of the 2.3-mm device. The maximum slope efficiency is 0.05 W/A with 0 V applied to the absorber. The inset of Fig. 6 demonstrates the optical spectrum under 170 mA DC bias on the gain section and −2 V applied to the absorber. The peak lasing wavelength is around 1.59-µm as described above. Figure 7 confirms that the mode-locked repetition rate is 18.4 GHz for the 2.3-mm device and shows the first two harmonics without any undesirable self-pulsation. Figure 8 corroborates that the fundamental mode-locked repetition rate is 12.3 GHz for the 3.5-mm device and shows that at least three harmonics are observed, again without self-pulsation. Both diagrams show at least two harmonics in the RF spectrum, which gives us confidence that the devices of 2.3-mm and 3.5-mm length are mode-locked as was established in [15,17]. The RF spectral analysis is relied upon to characterize the mode-locking because it is very difficult to build a second harmonic generation autocorrelator with the required sensitivity at 1.59 µm wavelength. From the measurement results of the RF spectrum (not shown), we confirm that the 4-mm device does not mode-lock, which substantiates our prediction from the cavity design guidelines derived above and described in Table 2.

#113021 - $15.00 USD Received 18 Jun 2009; revised 15 Sep 2009; accepted 6 Oct 2009; published 16 Oct 2009
(C) 2009 OSA

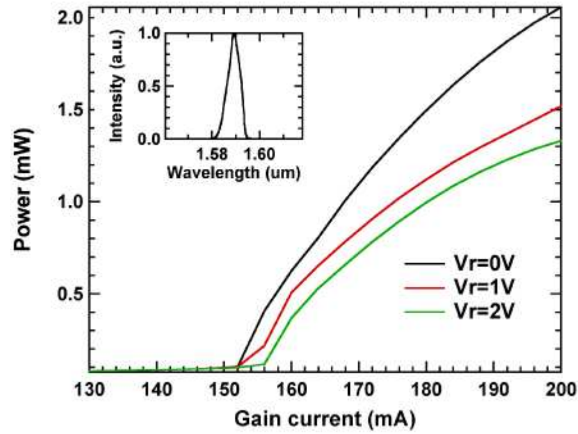

Fig. 6. L-I curve with reverse voltage from 0V to 2V of the 2.3-mm passive MLL. Inset: Optical spectrum with a DC gain current of 170 mA on the 2-mm gain section and a reverse voltage of 2V on the 0.3-mm absorber.

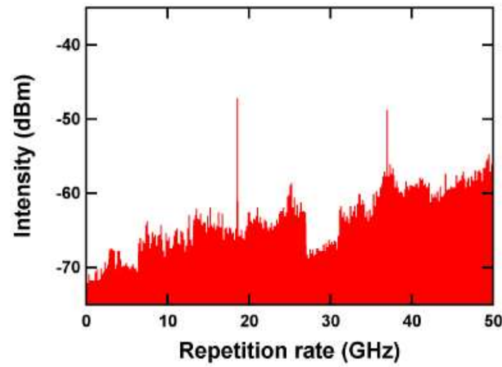

Fig. 7. The full span of the RF spectrum at 170mA and 2V reverse voltage of the 2.3-mm two-section passive QDash MLL device. The fundamental repetition frequency is 18.4 GHz. The RF spectrum clearly shows the first two harmonic components.

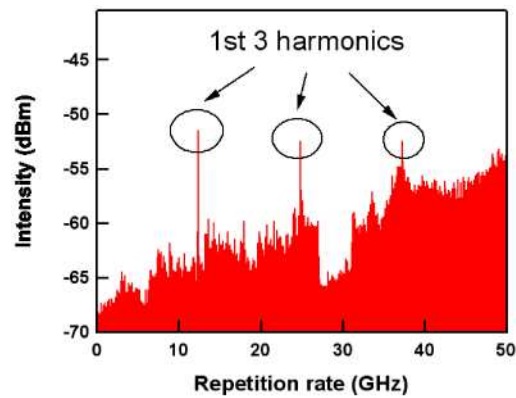

Fig. 8. The full span of the RF spectrum at 400mA and 1V reverse voltage of the 3.5-mm two-section passive QDash MLL device. The fundamental repetition frequency is 12.3 GHz. The RF spectrum clearly shows the first three harmonic components.

#113021 - $15.00 USD Received 18 Jun 2009; revised 15 Sep 2009; accepted 6 Oct 2009; published 16 Oct 2009
(C) 2009 OSA

5. Conclusion

Guidelines for mode-locking in two-section passive MLLs that have separate gain and saturable absorber regions and significant internal loss have been derived through the net-gain modulation phasor approach and applied to a variety of cavity designs for long-wavelength QDash MLLs. It has been shown that the new set of equations can be used to predict functional device layouts using measured modal gain and loss characteristics that are obtained through the segmented contact method on the *actual* device. After the modal gain and total loss measurement, the MLL was built by reconfiguring this same linear array of diodes. Equation (8) was found to be most useful when designing the two-section passive MLL cavities since it does not include the peak power, carrier lifetime and waveguide internal loss. From Table 2, it has been confirmed that Eq. (1) is not particularly instructive for designing two-section semiconductor MLLs. The experimental results corroborated the theoretical predictions, which should be an invaluable tool for future realization of long-wavelength passive QDash MLLs that are generally difficult to achieve.

Acknowledgments

The authors gratefully acknowledge sponsorship of this work from the U.S. Air Force Research Laboratory under Grant FA9550-06-1-0411 and program manager Dr. Gernot Pomrenke.

#113021 - $15.00 USD Received 18 Jun 2009; revised 15 Sep 2009; accepted 6 Oct 2009; published 16 Oct 2009
(C) 2009 OSA